Carrier confinement potential in quantum-well wires fabricated by implantation-enhanced interdiffusion in the GaAs-$Ga_{1-x}Al_xAs$ system

J. Cibert
Laboratoire de Spectrométrie Physique, Université Scientifique et Médicale de Grenoble, B.P.87, 38402 St. Martin d'Hères Cedex, France

P. M. Petroff
Materials Program and Department of Electrical Engineering, University of California, Santa Barbara, California 93106
(Received 29 January 1987)

We compute the shape of the confinement potential resulting from the interdiffusion of a GaAs quantum well locally enhanced by defects due to gallium implantation. We use the simplest model taking into account the lateral diffusion of the defects. A variational calculation of the first two electronic levels within this two-dimensional potential supports the assignment of the recently observed new cathodoluminescence lines to electrons laterally confined in a graded potential.

Enhancement of Ga-Al interdiffusion across the GaAs/$Ga_{1-x}Al_xAs$ interface is known to be an efficient method for locally altering the band gap of a quantum well (QW). Both the presence of impurities (Zn, Si, etc., either through implantion or diffusion[1]) and implantation damage[2] can enhance the interdiffusion. Recently,[3,4] damage due to Ga^+ implantation allowed fabrication of QW wires and QW boxes by using gold masks featuring arrays of wires and dots with sizes around 500 Å and above. New cathodoluminescence lines were observed on these structures and attributed to transitions involving electrons laterally confined in a potential graded in shape. As the shape of the potential determines the energies of the transitions, it is important to estimate the Al concentration profile (which determines the potential profile) resulting from the locally enhanced interdiffusion.

In this paper we develop the simplest possible model, taking explicitly into account the lateral diffusion during the annealing. Surprisingly, the interdiffusion profile can be calculated analytically: Hence an extension of this model to a large number of materials and to different processes should be contemplated. In this paper we shall restrict ourselves to the recently reported QW wires fabricated through implantation-enhanced interdiffusion of a GaAs QW, since quantitative data are available for this system. We show that the straggling during implantation and the lateral diffusion of the defects during the annealing are crucial and indeed lead to a graded profile for mask sizes between 500 and 2000 Å. A variational calculation of electron and hole levels within this (two-dimensional) potential semiquantitatively agrees with the cathodoluminescence results, and hence supports the interpretation given in Refs. 3 and 4. Finally, a few obviously needed refinements of the model are outlined.

As described in Refs. 3 and 4, the sample was a 50-Å GaAs QW sandwiched between two thick (500–900-Å) $Ga_{0.66}Al_{0.34}As$ barriers. A thick GaAs buffer layer prevented any diffusion of impurities from the [semi-insulating, (100), GaAs] substrate. The sample was implanted at room temperature with 5×10^{12}–5×10^{13} Ga^+ ions/cm^2, with a beam current lower than 1 μA/cm^2. A gold mask was deposited prior to implantation in order to define large implanted and nonimplanted pads and arrays of nonimplanted wires and dots with sizes ranging from 500–5000 Å. After removal of the mask the sample was annealed for a few seconds at 900–950 °C.

All calculations are done for a QW wire, but can be extended to the case of a QW box. We label z the direction perpendicular to the initial interface (Fig. 1), y the direction perpendicular to the wire. L_z (L_y) is the width of the initial QW (mask).

In Ref. 5 the interdiffusion enhancement was reported to saturate for long annealing times: This demonstrates that the enhancement is due to defects which are introduced during the implantation, and annealed during the high-temperature stage where the interdiffusion takes place. The nature of these defects is not known: A vacancy moving on the group-III sublattice[6,7] would be the

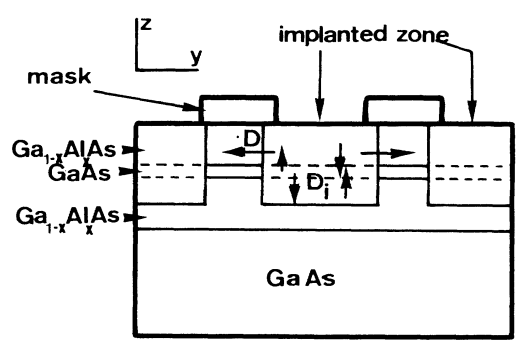

FIG. 1. Schematic of the diffusion modeling. The shaded area corresponds to the damage distribution due to the Ga^+ ion implantation. D is the diffusion coefficient for the defect which enhances the Ga-Al interdiffusion. D_i is the interdiffusion coefficient.

 ©1987 The American Physical Society

simplest hypothesis, but more complex defects or more complicated motions may be proposed. Considering the low doses used in the experiments (lower than the amorphization threshold), we shall assume that only elemental point defects are involved. Moreover we shall assume that only one kind of point defect is important, which can be described by its distribution. The initial defect distribution is defined by the mask profile (a square mask is assumed) and also by the ion straggling during implantation. The tabulated[8] projected range for 210-KeV Ga^+ ions implanted in GaAs is $R_p = 800$ Å and its deviation $\Delta R_p = 350$ Å. The damage distribution is estimated to be maximum around $0.7R_p$ with a width similar to ΔR_p. We will assume therefore a uniform damage distribution along the z direction (Fig. 1) in the vicinity of the QW, since $L_z = 50$ Å. We shall take a lateral variation in the defect distribution identical to the lateral variation of the implantation profile, i.e.,[9]

$$N(y,t=0)=N_0\left[1-\tfrac{1}{2}\mathrm{erf}\frac{\frac{1}{2}L_y-y}{\sigma}-\tfrac{1}{2}\mathrm{erf}\frac{\frac{1}{2}L_y+y}{\sigma}\right], \quad (1)$$

where σ is the lateral straggling, tabulated in Ref. 8 (multiplied by $\sqrt{2}$). This expression gives the defect density after implantation ($t=0$); during the high-temperature stage, the defects move and are annealed. We shall assume that their motion is described by a classical diffusion law with a diffusion coefficient D; this approximation will be discussed later. The diffusion along y smoothens the defect distribution, changing the width of the error function in Eq. (1) into $(\sigma^2+4Dt)^{1/2}$. The diffusion of the defects also plays a role in the decay of the defect density, either by trapping or by annihilating with other defects. In principle this is a stochastic process, and the microscopic nature of the motion has to be considered;[10] for short times we shall use a macroscopic equation and describe the decay of the defect density by a uniform time constant. This may appear as a rather crude approximation, and at least a dependence on the (local) implantation dose should be introduced. However, it can be justified if native defects (impurities, dislocations, or interfaces) are involved in the decay, or if, e.g., vacancies annihilate with interstitials (which are known to rapidly diffuse at low temperature and will hence be uniformly distributed when the vacancies begin to move). This approximation of a constant lifetime will be taken as purely phenomenological, with a time constant τ obtained from the annealing curve (see Fig. 2 of Ref. 5): Clearly the effect of the diffusion along z is included in τ. Then the defect density at time t during the high-temperature stage is given by

$$N(y,t)=N_0\left[1-\tfrac{1}{2}\mathrm{erf}\frac{\frac{1}{2}L_y-y}{(\sigma^2+4Dt)^{1/2}}-\tfrac{1}{2}\mathrm{erf}\frac{\frac{1}{2}L_y+y}{(\sigma^2+4Dt)^{1/2}}\right]e^{-t/\tau}. \quad (2)$$

The interdiffusion is induced by the motion of the defects across the interface. We describe it by a classical diffusion law, with an interdiffusion coefficient D_i proportional to the local defect density: $D_i(y,t)=\alpha DN(y,t)$, where α is a numerical factor which can be close to unity. Since D_i depends on the position across the wire, we have to use the second Fick's law to describe the evolution of the Al concentration $c(z,y,t)$:

$$\frac{\partial c(z,y,t)}{\partial t}=\frac{\partial D_i}{\partial y}\frac{\partial c}{\partial y}+D_i\frac{\partial^2 c}{\partial y^2}+D_i\frac{\partial^2 c}{\partial z^2}.$$

However, the scale involved in the variation of D_i (a few hundred Å) is large compared to the interdiffusion length (a few tens of Å). Hence the first two terms are negligible. That means that the interdiffusion at the center of the wire corresponds to a local Al-Ga exchange across the interface (due to defects moving first parallel to the interface, on a scale given by the defect diffusion length, and then intersecting the interface), and not to Al diffusing along y. The resulting Al concentration after annealing for a time t is given by

$$c(z,y,t)=c_0\left[1-\tfrac{1}{2}\mathrm{erf}\frac{\frac{1}{2}L_z-z}{2\Delta_i(y,t)}-\tfrac{1}{2}\mathrm{erf}\frac{\frac{1}{2}L_z+z}{2\Delta_i(y,t)}\right], \quad (3)$$

where c_0 is the initial Al concentration in the barrier, and $\Delta_i(y,t)$ the interdiffusion length, given by $\Delta_i^2(y,t)=\alpha D\int_0^t N(y,\theta)d\theta$. It turns out that for a long anneal (infinite t), the integral can be calculated analytically (see the Appendix). Its variation along y is determined by the mask profile, the straggling during implantation, and the diffusion length of the defect $\Delta=\sqrt{D\tau}$. The calculated interdiffusion length is plotted on Fig. 2 for two cases: (a) the diffusion length of the defect is small compared to the implantation straggling, and (b) the diffusion length is $\Delta=250$ Å. It is clear that the potential profile for a 1000-Å mask is far from being a square one. For smaller mask sizes, the width of the profile is not changed (it is mainly determined by the defect diffusion length and the implantation straggling), and the only change occurs in the amount of interdiffusion at the center of the wire: Qualitatively one expects a global shift of all electronic levels more than a change in their splittings. A flat bottom (trends toward a square profile) is observed only for masks wider than 2500 Å if $\Delta=250$ Å. This value of the defect diffusion length is not arbitrary: with an effective defect lifetime $\tau\approx 10$ s (measured on a plot similar to Fig.

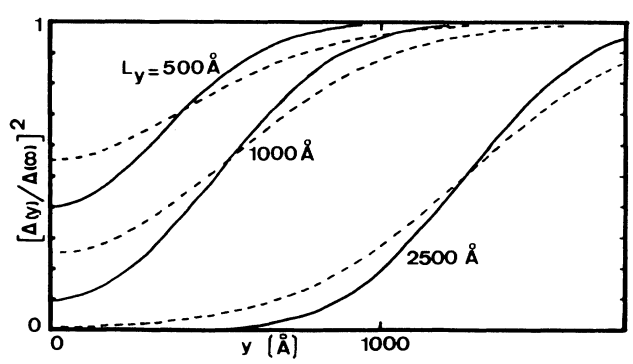

FIG. 2. Squared interdiffusion length (normalized to its value far from the mask) as a function of the position across the wire. Mask width: $L_y = 500, 1000, 2500$ Å. Diffusion length of the defects: negligible (solid line) or 250 Å (dashed line).

2 of Ref. 5), the defect diffusion coefficient is $D=6\times10^{-13}$ cm^2/s. In Ref. 11, lateral diffusion was measured by transmission electron microscopy after a long anneal at 800 °C, with the estimate $D(800\,°\mathrm{C})=(4-9)\times10^{-14}$ cm^2/s (this must be considered as a maximum value since it was obtained from the motion of the point where complete interdiffusion of a superlattice occurred); an increase by a factor of 10 (or lower) between 800 and 900 °C (i.e., an activation energy smaller than 2.3 eV) is reasonable. Moreover in our model the ratio of the maximum interdiffusion length (far from any mask) to the defect diffusion length is $\sqrt{\alpha N_0}$; from the luminescence shift observed on uniformly implanted parts of the sample,[3,4] and using the calculated energy levels in an interdiffused QW (Fig. 3), we get $\Delta_i=11$ Å after annealing at 900 °C. Hence $\alpha N_0\approx2\times10^{-3}$, i.e., approximately ten effective defects per implanted ion if $\alpha=1$.

The electronic energy levels within the two-dimensional potentials $V(z,y)=750c(z,y)$ (in meV, for electrons) or $V(z,y)=500c(z,y)$ (for holes), where $c(z,y)$ is given by Eq. (3) and $\Delta_i(y)$ is calculated in the Appendix, were evaluated using a variational method. The anisotropy of the hole mass (and the coupling between heavy holes and light holes) and its dependence on the aluminum concentration were neglected: hence electrons and holes are simple particles with isotropic masses $m_e=0.067m_0$ and $m_h=0.45m_0$. The test functions were Gaussian functions, $\exp[-(az^2+by^2)]$ and $y\exp[-(az^2+by^2)]$, which give surprisingly accurate results for the confinement energy along z (Fig. 3) and are expected to be a good approximation for the graded lateral potential since they are the exact wave functions in a harmonic potential. The width of the Gaussian function (i.e., a and b) was taken as the variational parameter and was adjusted separately for electrons and holes until the total energy was minimized. The transitions corresponding to the first two levels are plotted in Fig. 4 as a function of the mask size. The main features are the splitting (about 4 meV in the 500–2000 Å range, to be compared to 5–8 meV experimentally), and the shift, vanishing above 3000 Å only, which is mainly due to interdiffusion over the whole wire and only for a small part to the lateral quantization.

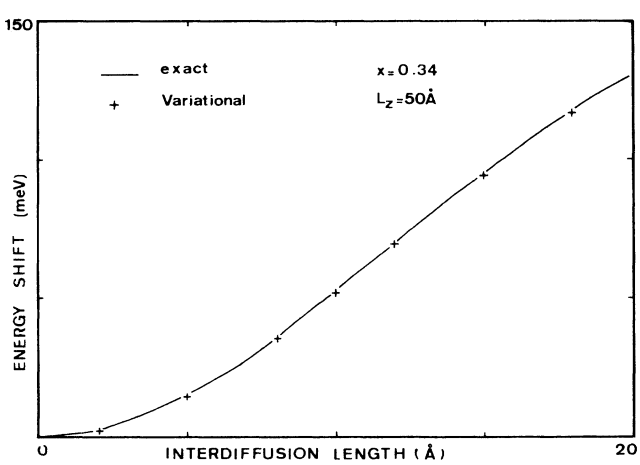

FIG. 3. Energy shift of the transition between the first electron and hole levels of an interdiffused QW vs the interdiffusion length. Solid line, exact calculation; crosses, variational calculation.

We must emphasize that the model developed here is a first step towards the description of QW wires obtained through local interdiffusion of a two-dimensional QW: It is in fact the simplest model taking into account the real defect distribution during the high-temperature stage. The worse approximations are probably (a) the recourse to an effective lifetime to describe the annealing of the defects and (b) the description of their motion by a classical diffusion law with a single diffusion coefficient. In fact there is some experimental evidence[11] that the hopping rates for Ga and Al are different: This will alter the interdiffusion profile.[12] Finally a precise calculation of the energy levels remains to be done: The variational method is probably not too much in error, but a correct description of the valence band should be used, including the coupling between heavy holes and light holes.

As a conclusion we present a calculation of the profile expected for QW wires obtained through interdiffusion of a two-dimensional QW locally enhanced by implantation. We use the simplest possible model taking into account the distribution and the motion of the defects which enhance the interdiffusion. The lateral profile of the potential is clearly graded for masks narrower than 2000 Å, its width being determined by the lateral implantation straggling and the diffusion length of the defects. A variational calculation of the energy of transitions involving the first two electronic levels semiquantitatively accounts for the shifts and splittings of the cathodoluminescence lines reported in Refs. 3 and 4. These experiments are representative of a rapidly expanding field of researches, where a two-dimensional semiconductor structure is locally altered in order to confine the carriers to one or zero dimensions. The fact that we obtain an analytical expression for the interdiffusion profile should allow an easy extension of our calculation to many practical cases.

APPENDIX

The interdiffusion profile after a long anneal ($t\gg10$ s) is given by Eq. (3) with

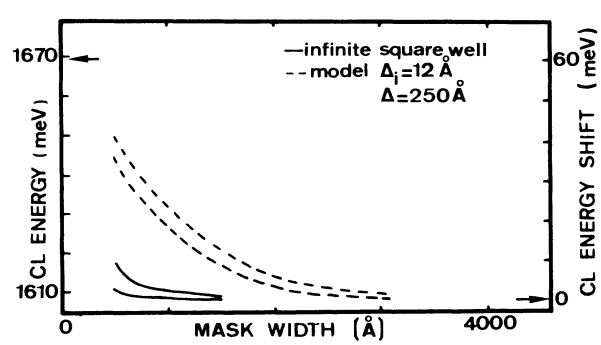

FIG. 4. Energy of the cathodoluminescence (CL) transition involving the first two levels of electrons and holes laterally confined in a QW wire vs the mask width.

$$\Delta i^2(y)=\alpha N_0 D\tau[J(\tfrac{1}{2}L_y-y)+J(\tfrac{1}{2}L_y+y)] \ , \qquad \text{(A1)}$$

where

$$J(X)=\frac{1}{\tau}\int_0^\infty dt\, e^{-t/\tau}\int_{X/(\sigma^2+4Dt)^{1/2}}^\infty e^{-\alpha^2}d\alpha \ .$$

The error function in Eq. (3) is replaced here by its integral definition. Obviously each of the two J functions corresponds to one edge of the mask.

We first separate the effect of straggling from the effect of diffusion by using the properties of Gaussian functions with respect to convolution; hence,

$$J(X)=\frac{1}{\tau}\int_0^\infty dt\, e^{-t/\tau}\frac{1}{\pi\sigma\sqrt{4Dt}}\int_X^\infty d\alpha\int_{-\infty}^\infty d\beta \exp\left[-\left[\frac{\beta^2}{4Dt}+\frac{(\alpha-\beta)^2}{\sigma^2}\right]\right] .$$

Permuting the integrals, and using[13]

$$\frac{1}{\tau\sqrt{\pi}}\int_0^\infty dt\, e^{-t/\tau}\frac{1}{\sqrt{4Dt}}e^{-\beta^2/4Dt}=\frac{1}{\sqrt{4D\tau}}e^{-\beta/\sqrt{D\tau}}$$

(valid if $\beta\geq 0$), we obtain

$$J(X)=\frac{2}{\sigma\sqrt{\pi D\tau}}\int_X^\infty d\alpha\int_0^\infty d\beta\, e^{-\beta/\sqrt{D\tau}}\frac{1}{2}\left\{\exp\left[-\left[\frac{\alpha+\beta}{\sigma}\right]^2\right]+\exp\left[-\left[\frac{\alpha-\beta}{\sigma}\right]^2\right]\right\} .$$

It is now straightforward to calculate the first term using $(\alpha+\beta)$ as a new variable (and the second one using $\alpha-\beta$), with the result

$$J(X)=\tfrac{1}{2}\mathrm{erfc}\left[\frac{x}{\sigma}\right]-\tfrac{1}{4}e^{-\sigma^2/4D\tau}\left[e^{x/\sqrt{D\tau}}\mathrm{erfc}\left[\frac{\sigma}{\sqrt{4D\tau}}+\frac{X}{\sigma}\right]-e^{-x/\sqrt{D\tau}}\mathrm{erfc}\left[\frac{\sigma}{\sqrt{4D\tau}}-\frac{X}{\sigma}\right]\right] ,$$

with $\mathrm{erfc}\,(A)=2/\sqrt{\pi}\int_A^\infty e^{-\alpha^2}d\alpha$.

This expression and Eqs. (A1) and (3) define the interdiffusion profile.

[1]W. D. Laidig, N. Holonyak, M. D. Camras, K. Hess, J. J. Coleman, P. D. Dapkus, and J. Bardeen, Appl. Phys. Lett. **38**, 776 (1981).

[2]Y. Hirayama, Y. Suzuki, S. Tarucha, and H. Okamoto, Jpn. J. Appl. Phys. **24**, L516 (1985).

[3]J. Cibert, P. M. Petroff, G. J. Dolan, S. J. Pearton, A. C. Gossard, and J. H. English, Appl. Phys. Lett. **49**, 1275 (1986).

[4]J. Cibert, P. M. Petroff, G. J. Dolan, D. J. Werder, S. J. Pearton, A. C. Gossard, and J. H. English, Second International Conference on Superlattices, Microstructures, and Microdevices, Goteborg, 1986, [Superlattices and Microstructures **3**, 35 (1987)].

[5]J. Cibert, P. M. Petroff, D. J. Werder, S. J. Pearton, A. C. Gossard, and J. H. English, Appl. Phys. Lett. **49**, 223 (1986).

[6]B. Goldstein, Phys. Rev. **121**, 1305 (1961).

[7]D. G. Deppe, L. J. Guido, N. Holonyak, Jr., K. C. Hsieh, R. D. Burnham, R. L. Thornton, and T. L. Paoli, Appl. Phys. Lett. **49**, 510 (1986).

[8]J. F. Gibbons, W. S. Johnson, and S. W. Mylroie, *Range Statistics in Semiconductors* (Academic, New York, 1975).

[9]S. Furukawa, H. Matsumura, and H. Ishiwara, Jpn. J. Appl. Phys. **11**, 134 (1972).

[10]G. Zumofen, A. Blumen, and J. Klafter, J. Chem. Phys. **82**, 3198 (1985).

[11]Y. Hirayama, Y. Suzuki, and H. Okamoto, Surf. Sci. **174**, 198 (1986).

[12]R. G. Walker and C. D. Wilkinson, Appl. Opt. **22**, 1929 (1983).

[13]*Table of Integrals, Series, and Products,* edited by I. S. Gradshteyn and I. M. Ryzhik (Academic, New York, 1980), p. 307, Eq. (3–325).